


# Oral Administration of Therapeutic Enzyme Capsule for the Management of Inflammatory Bowel Disease

Xiao Liang, Kai Wen, Yingxuan Chen, Guangxu Fang, Shengcai Yang, Quanshun Li 

Key Laboratory for Molecular Enzymology and Engineering of Ministry of Education, School of Life Sciences, Jilin University, Changchun, People's Republic of China

Correspondence: Quanshun Li; Shengcai Yang, Tel/Fax +86-431-85155200, Email quanshun@jlu.edu.cn; yang\_shengcai1990@163.com

**Background:** Oral administration of proteins/peptides is challenging in clinical application due to their instability and susceptibility in the gastrointestinal tract.

**Materials and Methods:** The in situ polymerization on the surface of enzymes was used to encapsulate antioxidant enzymes (superoxide dismutase (SOD) and catalase (CAT)) in polymeric shells, and the reactive oxygen species (ROS) scavenging ability was monitored based on DCFH-DA probe using flow cytometry and confocal laser scanning microscopy. The mRNA expression level of pro-inflammatory factors was assessed by real-time qPCR, using lipopolysaccharide-induced RAW264.7 cells as a model. Finally, the enzyme capsules were orally administered for the treatment of inflammatory bowel disease using dextran sodium sulfate (DSS)-induced colitis mice as a model, based on the evaluation of the disease-associated index, ROS level and pro-inflammatory cytokines' expression.

**Results:** The enzyme capsules could effectively scavenge the intracellular reactive oxygen species (ROS) through the cascade catalysis of SOD and CAT, and thus protect the cells from ROS-induced oxidative damage. Meanwhile, the enzyme capsules could inhibit the secretion of pro-inflammatory cytokines from macrophages, thereby achieving favorable anti-inflammation effect. Oral administration of enzyme capsules could facilitate the accumulation of enzymes in the inflamed colon tissues of DSS-induced colitis mice. Moreover, the oral delivery of enzyme capsules could effectively alleviate the symptoms associated with colitis, attributing to the excellent ROS scavenging ability and the inhibition of pro-inflammatory cytokines' level.

**Conclusion:** In summary, our findings provided a promising approach to construct enzyme-based nano-formulations with favorable therapeutic efficacy and biocompatibility, exhibiting great potential in the treatment of gastrointestinal diseases in an oral administration manner.

**Keywords:** antioxidant enzymes, in situ polymerization, oral administration, reactive oxygen species, anti-inflammation, colitis

## Introduction

Inflammatory bowel disease (IBD), including crohn's disease and ulcerative colitis, is a chronic recurrent idiopathic immune disease of gastrointestinal tract.<sup>1,2</sup> IBD is characterized with intestinal immune dysregulation, epithelial barrier dysfunction and intestinal ulcers in the ileum, rectum and colon,<sup>3</sup> which has been identified to be associated with multiple factors, such as genetic, bacterial and environmental ones.<sup>4-7</sup> The most direct contributor to intestinal damage is the overproduction of reactive oxygen species (ROS) including hydrogen peroxide ( $H_2O_2$ ), superoxide anion ( $\bullet O_2^-$ ) and hydroxyl radical ( $\bullet OH$ ), which can serve as an inflammatory mediator and facilitate the progression of inflammation.<sup>8,9</sup> Thus, ROS-mediated oxidative stress is closely associated with the etiology of IBD,<sup>10</sup> and removing excessive intracellular ROS or blocking the production of ROS has been demonstrated to be an effective strategy for the IBD treatment.<sup>11-13</sup>

In recent years, exogenous supplementation of antioxidant enzymes has become a reasonable and effective therapeutic approach to reduce ROS level, showing great potential in the prevention or treatment of inflammatory

diseases.<sup>14–16</sup> Superoxide dismutase (SOD) and catalase (CAT) are two major antioxidant enzymes in humans, serving as cascade catalysts for the ROS scavenging. SOD scavenges  $\bullet\text{O}_2^-$  by converting this free radical to  $\text{H}_2\text{O}_2$ , and the original or produced  $\text{H}_2\text{O}_2$  will be converted to  $\text{H}_2\text{O}$  and  $\text{O}_2$  under the CAT catalysis, which can effectively scavenge ROS and prevent the oxidative damage to tissues and cells. However, SOD (usually in the mitochondria or cell membrane) and CAT (usually in the peroxisome) are not located in the same subcellular compartment, which means that an additional transportation step is required between the production and degradation of  $\text{H}_2\text{O}_2$ .<sup>17–19</sup> To address this issue, it is necessary to transport these two enzymes in the same subcellular compartment to achieve the exogenous supplementation of therapeutic enzymes in a synergistic manner, thereby obtaining higher efficiency than the native system.

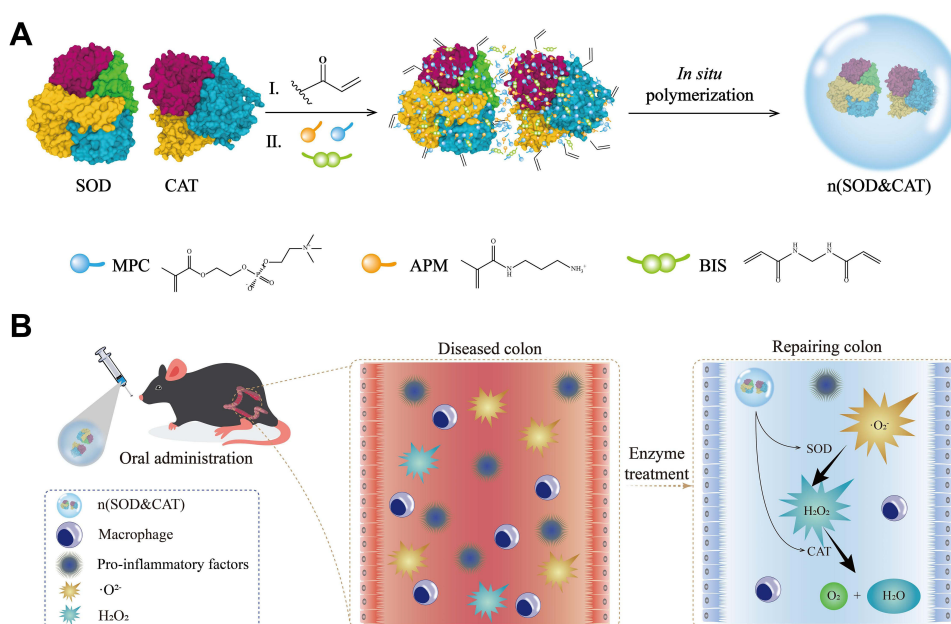
To date, oral administration with minimal systemic exposure and immunosuppression has been considered to be the best choice in the delivery of therapeutic proteins to the inflamed intestinal site.<sup>20</sup> Oral administration has the advantages of convenience, simplicity, minimal pain and high applicability, especially for the treatment of chronic diseases.<sup>21</sup> Meanwhile, it is expected to solve the non-compliance problem of protein and peptide molecules during the injection.<sup>22</sup> However, it is still challenging to achieve high efficacy in the oral administration of proteins, owing to the acidic environment and pepsin in the stomach. In addition, high molecular weight and poor permeability of proteins hamper the efficacy of oral administration.<sup>8,23</sup> Hence, there is an urgent need to construct efficient strategies for realizing the oral delivery of therapeutic proteins. Up to now, various strategies have been reported to overcome the undesirable degradation and the changes of original structure or bioactivity of enzymes,<sup>24,25</sup> such as the wind chimes-like cyclodextrin to encapsulate natural anti-inflammatory proteins<sup>12</sup> and the biodegradable methoxy-poly(ethylene glycol)-block-poly (L-lactide) microspheres to execute the oral delivery of insulin.<sup>26</sup> Recently, in situ polymerization of biomacromolecules has been demonstrated to be an emerging technology to construct polymer-biomacromolecule nanocomposites.<sup>27,28</sup> This strategy could enhance the stability of biomacromolecules in the physiological and non-physiological environment, and has been widely used in the oral or intravenous administration of a series of proteins.<sup>29–32</sup>

Herein, antioxidant enzymes SOD and CAT were encapsulated within polymer shells by the surface-initiated in situ polymerization reaction to obtain therapeutic capsule n(SOD&CAT), which was then applied in the oral administration to achieve the IBD treatment (Scheme 1). This thin polymeric shell could protect the loaded proteins from the degradation in the environment of gastric acid and pepsin, thereby maintaining favorable enzymatic activity and allowing the rapid ROS scavenging. After evaluating the stability, the ROS scavenging and in vivo anti-inflammation ability of n(SOD&CAT) capsule after the oral administration was investigated using dextran sodium sulfate (DSS)-induced colitis mice as a model.

## Materials and Methods

### Materials

SOD from bovine erythrocytes and CAT from bovine liver were acquired in Biodee Co. (Beijing, China). *N*-acryloxysuccinimide (NAS), bisacrylamide (BIS), *N*-(3-aminopropyl) methacrylamide hydrochloride (APM), ammonium persulfate (APS), *N,N,N',N'*-tetramethylethylenediamine (TEMED) and 2-methacryloyloxyethyl phosphorylcholine (MPC) were supplied by Sigma-Aldrich (Shanghai, China). Rhodamine B isothiocyanate (RBITC) and all the primers were obtained from Sangon Biotech. (Shanghai, China). 3-(4,5-Dimethylthiazol-2-yl)-2,5-diphenyltetrazolium bromide (MTT) was purchased from Amresco (Solon, OH, USA). Lipopolysaccharide (LPS), phenyl-Sepharose CL-4B column, hydroxyl free radical assay kit and superoxide anion assay kit were purchased from Solarbio (Beijing, China). Dulbecco's modified Eagle's medium (DMEM) and fetal bovine serum (FBS) were purchased from Gibco (Grand Island, MO, USA). Dextran sodium sulfate (DSS, 40 kDa) was supplied by Aladdin (Shanghai, China). The dye 2,7-dichlorofluorescein diacetate (DCFH-DA), assay kits for SOD and CAT activities, and malondialdehyde (MDA) detection kit were purchased from Beyotime (Shanghai, China). TRIzol universal reagent and myeloperoxidase (MPO) detection kit were acquired from JianCheng Bioengineering Institute (Nanjing, China) and TIANGEN Biotech. Co. (Beijing, China), respectively. SYBR Premix Ex Taq kit and PrimeScript<sup>TM</sup> RT reagent kit were obtained from TaKaRa (Dalian, China). Enzyme-linked immunosorbent assay (ELISA) kits for mouse CCL2, IL-6 and TNF- $\alpha$  were purchased from Cloud-Clone Co. (Wuhan, China). Bicinchoninic acid (BCA) protein assay kit and trypsin were purchased from BioTeke Co. (Beijing,



**Scheme 1** (A) Preparation of n(SOD&CAT) capsule by in situ polymerization around therapeutic enzymes SOD and CAT. (B) Oral administration of n(SOD&CAT) capsule to scavenge ROS for the colitis treatment.

China) and Gentihold Co. (Beijing, China), respectively. Unless otherwise mentioned, all the reagents were used without additional purification.

## Preparation and Characterization of n(SOD), n(CAT) and n(SOD&CAT)

The n(SOD&CAT) capsule was prepared according to a previously reported protocol with some modifications.<sup>32</sup> Briefly, SOD (5 mg), CAT (10 mg) and NAS (0.25 mg) were subjected to reaction at 4 °C for 2 h (1:20:40, w/w/w, NAS: SOD: CAT), and then the mixture was dialyzed through a membrane of MWCO 3500 against PBS (50 mM, pH 7.4) at 4 °C overnight to obtain the acrylate-modified proteins. MPC (240 mg), APM (16 mg) and BIS (14 mg) (240:16:14:5:10, w/w/w/w/w, MPC: APM: BIS: SOD: CAT) were added to the above acrylate-modified SOD&CAT solution. Further, APS (5 mg) and TEMED (12 µL) were used to trigger the initiation of polymerization. The sample was stirred at 4 °C for 2 h, dialyzed using a membrane of MWCO 3500 Da against PBS (50 mM, pH 7.4) and purified using a phenyl-Sepharose CL-4B column to obtain n (SOD&CAT) solution through the elution of PBS buffer (10×). The specific activities of these two components in n (SOD&CAT) capsule were measured using the corresponding activity detection kits. The n(SOD) and n(CAT) capsules were prepared using a similar protocol. Transmission electron microscopic (TEM) images of n(SOD), n(CAT) and n (SOD&CAT) were captured on a HITACHI-H800 microscope (Tokyo, Japan) at an accelerating voltage of 200 kV. The hydrodynamic diameter and zeta potential of these capsules were measured by Malvern Nano ZS90 Zetasizer (Malvern, UK). The SDS-PAGE analysis was conducted on 12% polyacrylamide gel with 20 µg protein per well (120 V, 120 min). Far ultraviolet circular dichroism (CD) spectra were recorded on a JASCO-810 circular dichroism spectrometer (JASCO Inc., Tokyo, Japan) in the wavelength range of 190–250 nm at a scanning speed of 100 nm/min.

## Enzyme Activity and Stability Analysis

The antioxidant activities of SOD and CAT were measured by the corresponding assay kits. The SOD activity was calculated according to the superoxide radical-dependent formazan dye reduction, monitoring at 450 nm by HBS-1096A microplate reader (Nanjing, China). The CAT activity was performed based on the reduced absorbance at 520 nm due to the ability to scavenge H<sub>2</sub>O<sub>2</sub>, and the activity was converted from the speed of H<sub>2</sub>O<sub>2</sub> consumption. Enzyme activity was expressed as the percentage of the control group. The thermal stability of n(SOD) and n(CAT) was evaluated by the incubation of these samples in PBS (50 mM, pH 7.4) at 40 °C for 24 h. The proteolytic stability was

detected through the incubation with trypsin (50 µg/mL) at 37 °C for 30 min, and the stability under acidic conditions was measured in PBS solution (50 mM, pH 2.0) at 37 °C for 4 h. For all the stability studies, the final concentration of n(SOD) and n(CAT) was 200 µg/mL, and the residual activity was measured by the corresponding assay kits at predetermined time points. Native SOD and CAT with the same concentration were treated under the same conditions and used as the control. Data were expressed as mean residual activity  $\pm$  standard deviation (SD) of triplicate experiments.

## Free Radical Scavenging Ability Assay

The scavenging ability of  $\text{H}_2\text{O}_2$ ,  $\cdot\text{O}^{2-}$  and  $\cdot\text{OH}$  was analyzed using the corresponding assay kits based on the manufacturer's protocols. For the  $\text{H}_2\text{O}_2$  scavenging activity, SOD, n(SOD), CAT, n(CAT), SOD+CAT, n(SOD)+n(CAT) or n(SOD&CAT) (SOD: 100 µg/mL, CAT: 100 µg/mL) were incubated with 100 mM of  $\text{H}_2\text{O}_2$  at 37 °C for 20 min, and the amount of  $\text{H}_2\text{O}_2$  remaining in the reaction system was measured by the CAT assay kit. For the  $\cdot\text{O}^{2-}$  scavenging ability, APS-TEMED system was utilized to generate  $\cdot\text{O}^{2-}$ , which could react with hydroxylamine hydrochloride to form  $\text{NO}_2^-$ , and then the produced  $\text{NO}_2^-$  reacted with *p*-aminobenzenesulfonic acid and  $\alpha$ -naphthylamine to generate a red azo compound (characteristic absorbance at 530 nm). Different formulations (SOD: 100 µg/mL, CAT: 100 µg/mL) were incubated with  $\cdot\text{O}^{2-}$  at 37 °C for 30 min, and the absorbance values at 530 nm were measured which were negatively correlated to the  $\cdot\text{O}^{2-}$  scavenging ability. For the  $\cdot\text{OH}$  scavenging activity, the Fenton reaction of  $\text{H}_2\text{O}_2/\text{Fe}^{2+}$  ( $\text{Fe}^{2+} + \text{H}_2\text{O}_2 \rightarrow \text{Fe}^{3+} + \cdot\text{OH} + \text{OH}^-$ ) was applied to generate  $\cdot\text{OH}$  which further oxidized  $\text{Fe}^{2+}$  to  $\text{Fe}^{3+}$ . Only  $\text{Fe}^{2+}$  could combine with 1.10-phenanthroline to obtain a red product 1.10-phenanthroline- $\text{Fe}^{2+}$  (maximum absorbance at 536 nm), and thus the inhibition of decreasing rate of absorbance values at 536 nm could be used to represent the  $\cdot\text{OH}$  scavenging ability. After the incubation of different formulations (SOD: 100 µg/mL; CAT: 100 µg/mL) with  $\cdot\text{OH}$  at 37 °C for 30 min, the absorbance at 536 nm were measured to calculate the  $\cdot\text{OH}$  scavenging rate according to the previous report.<sup>33</sup>

## Cytotoxicity Assay of n(SOD) and n(CAT) Capsules

Human colorectal cancer cell lines (SW480 and HCT116) and macrophage cell line RAW264.7 were obtained from Shanghai Institute of Cell Bank (Shanghai, China). SW480 and HCT116 cells were cultured in DMEM containing 10% FBS and 1% penicillin-streptomycin at 37 °C under 5%  $\text{CO}_2$ . The cells were seeded in 96-well plates (density:  $8.0 \times 10^3$  cells/well) and cultured overnight. Then n(SOD) or n(CAT) capsules with different concentrations (0–500 µg/mL) were added into the wells in the plates. After the incubation at 37 °C for 24 h, the cell viability was measured by standard MTT assay.<sup>34</sup>

## ROS Scavenging and Cell Protection Capacity Analysis

To detect the ROS scavenging ability of different capsules, SW480 cells were seeded in 6-well plates ( $2.5 \times 10^5$  per well) and incubated at 37 °C for 12 h. Then different formulations (SOD: 5 µg/mL, CAT: 10 µg/mL) were added into the wells to treat the cells for 12 h. Then DCFH-DA (0.01 mM) in DMEM was added into the wells followed by the incubation for 30 min. Rosup was used to treat the samples for 24 h (final concentration of 1 mg/mL). To quantify the intracellular ROS, the cells were harvested, washed with PBS twice and analyzed by CytoFLEX flow cytometer (Beckman Coulter Inc.) at the excitation and emission wavelengths of 488 and 525 nm, respectively. In addition, the intracellular ROS level was detected by confocal laser scanning microscopy (CLSM, Carl Zeiss Microscopy LLC, Jena, Germany), in which the cells were inoculated into the coverslips in each well and treated as above. To verify the ability of formulations to prevent the oxidative damage, SW480 and HCT116 cells were preincubated with different formulations for 12 h (SOD: 5 µg/mL, CAT: 10 µg/mL) and then treated with Rosup (1 mg/mL) for 24 h, and the cell viability was measured by standard MTT assay.<sup>34</sup>

## In vitro Anti-Inflammation Ability

Briefly, macrophage RAW264.7 cells were inoculated in 2 mL 10% FBS-containing DMEM in 6-well plates at a density of  $2.5 \times 10^5$  cells/well and cultured overnight. The cells were subsequently treated with different formulations (SOD: 5 µg/mL,



CAT: 10 µg/mL) for 12 h, washed with PBS three times and stimulated with LPS (100 ng/mL) for 24 h. Then the cells were collected to extract total RNA using TRIzol reagent. Total RNA (1.0 µg) was reversely transcribed to cDNA, and real-time qPCR analysis was performed to measure the expression level of inflammation-related factors (TNF-α, IL-6 and CCL2) on an ABI 7500 Fast Real-Time PCR System (Life Science, Foster, CA). The expression level was calculated through  $2^{-\Delta\Delta CT}$  method, in which β-actin was used as an internal reference. The sequences of primers were listed in [Table S1](#).

## Biodistribution Analysis

SOD was labelled with the dye RBITC, which was then used to visualize the in vivo biodistribution of therapeutic enzymes. Briefly, SOD (10 mg) was mixed with 10 mg of RBITC solution, and the reaction mixture was stirred at 4 °C in the dark overnight. The resulting product was purified by the dialysis (MWCO: 3500 Da) in distilled water, lyophilized and stored in -20 °C.

The animal studies were conducted according to the “Guide for the Care and Use of Laboratory Animals” (8th edition, International Publication No: 978-0-309-15400-0) and approved by the Institutional Animals Ethics Committee of Jilin University (license No. JSDF: 2021-PZ019). Male C57BL/6N mice (6 weeks old, ~18 g) were obtained from Vital River Laboratory Animal Technology Co. Ltd. (Beijing, China) and raised in a specific pathogen-free animal lab. The colitis mice were constructed by the usage of DSS (3%, w/v) in drinking water for 3 days. After the oral administration of RBITC-SOD or n(RBITC-SOD) at a dose of 5 mg/kg, the mice (n=3 per group) were sacrificed at predetermined time points (2, 4 and 12 h), and the major organs (colon, heart, liver, spleen, lung, stomach and kidney) were excised to capture the fluorescence images by IVIS Lumina XR in vivo imaging system (Xenogen Inc.) at excitation and emission wavelengths of 540 nm and 625 nm, respectively.

## In vivo Therapeutic Effect Against DSS-Induced Colitis Model

Male C57BL/6N mice were randomly divided into 5 groups (n=6 per group) and acclimated for 1 week before the experiment: Group 1, healthy mice; Group 2, 3% DSS + Saline; Group 3, 3% DSS + native SOD and CAT combination treatment; Group 4, 3% DSS + n(SOD)+n(CAT) combination treatment; Group 5, 3% DSS + n(SOD&CAT) treatment. For Group 1, the mice received normal drinking water during the experiment and used as a negative control group. For the other 4 groups, the mice received 3% DSS (w/v) in drinking water for 7 days to establish the model of colitis. Meanwhile, the mice were orally administered with different formulations on Day 1, 3, 5 and 7 (SOD: 3 mg/kg, CAT: 6 mg/kg), and the changes of body weight were monitored daily during the experiment. The disease-associated index (DAI) in mice was recorded daily according to the following parameters: changes in fecal consistency index (0–4), weight loss index (0–4) and fecal bleeding index (0–4).<sup>12</sup> The mice were subjected to fasting on Day 7, and then sacrificed on Day 8. The entire colons were collected and washed with saline gently, and the length of colons was measured. Meanwhile, major organs (heart, liver, spleen, lung and kidney) were collected and the organ indexes were calculated through the following formula.

$$\text{Organ index (\%)} = \text{weight of organ (g)} / \text{mice body weight (g)} \times 100\%$$

For hematoxylin and eosin (H&E) staining analysis, colonic tissues and major organs were fixed in 4% paraformaldehyde for 24 h, and the slices were photographed with an Olympus IX71 fluorescence microscope at a magnification of ×200 (Tokyo, Japan). Based on the Colonic Mucosa Damage Index (CMDI) standard,<sup>35</sup> the damage indexes were scored as follows: 0, no damage; 1, hyperaemia, no ulcers; 2, hyperaemia and thickening of the bowel wall, no ulcers; 3, one ulcer without thickened bowel wall; 4, two or more sites of ulceration/inflammation; 5, two or more major sites of ulceration and inflammation or one site of ulceration/inflammation extended >1 cm along the length of the colon.

## ROS Scavenging and Therapeutic Capacity Analysis in Colon Tissues

The ROS level in colon tissues was measured by DCFH-DA dye and quantified by flow cytometry. Briefly, the middle colon of each mouse was homogenized in PBS (50 mM) and incubated with DCFH-DA (0.01 mM) for 30 min. Afterward the sample was centrifuged at 2000 rpm for 5 min, and the cells were washed with PBS twice and subjected to the analysis on a CytoFLEX flow cytometer (Beckman Coulter Inc.). In addition, 50 mg of colonic tissues were homogenized with 1 mL PBS (50 mM), and the homogenate was centrifuged at 3000 rpm for 15 min to obtain the

supernatant. The levels of MPO and MDA in the supernatant were determined by the corresponding kits according to the manufacturers' instructions. Another 50 mg of colonic tissues of each mouse was homogenized at 4 °C and centrifuged at 3000 rpm for 15 min, and the SOD and CAT activities in the supernatants were determined by the corresponding assay kits.

## Expression Analysis of Pro-Inflammatory Cytokines in Colon Tissues

The expression of pro-inflammatory factors (IL-6, TNF- $\alpha$  and CCL2) in colonic homogenates were assessed by ELISA and qPCR assay. For ELISA assay, middle colon of each mouse was weighed and homogenized in lysate at 4 °C. The resulting homogenate was then centrifuged at 3000 rpm for 15 min (4 °C), and the supernatant was collected for the measurement by commercial mouse ELISA kits according to the manufacturer's instructions. Three samples per group were used for the quantitative analysis. In addition, the colonic tissues were homogenized with TRIzol reagent to extract total RNA and the mRNA levels of IL-6, TNF- $\alpha$  and CCL2 were quantified using qPCR.

## Biocompatibility Analysis

To evaluate the biocompatibility of enzyme capsules, the blood samples were collected on Day 8 and centrifuged at 3000 rpm for 10 min, and the supernatants were subjected to the measurement of serum biochemical indicators including aspartate transaminase (AST), alanine aminotransferase (ALT), alkaline phosphatase (ALP), blood urea nitrogen (BUN) and creatinine (CREA) on an Olympus AU-400 Automatic Biochemistry Analyzer.

## Statistical Analysis

Data were analyzed for statistical significance using Student's *t*-test by GraphPad Prism 8 (n.s., not significant; \**p* < 0.05; \*\**p* < 0.01; \*\*\**p* < 0.001).

## Results and Discussion

### Preparation and Characterization of Enzyme Capsules

The antioxidant enzymes SOD and CAT were encapsulated within polymer shells by surface-initiated in situ polymerization reaction to obtain therapeutic enzyme capsule n(SOD&CAT). As shown in [Scheme 1A](#), the polymerizable anchors were obtained by a mild vinylation reaction between NAS and the amine groups of lysine residues of SOD and CAT surface, and MPC and APM were used as monomers in the in situ polymerization. Meanwhile, BIS was served as crosslinkers to stabilize the encapsulated proteins. Firstly, these monomers and crosslinkers congregated around the proteins via non-covalent interactions (electrostatic interaction and hydrogen bonding). Then the in situ polymerization was initiated by APS and TEMED, and a thin and permeable "mesh-like" network of polymeric shell was formed around the enzymes to obtain the capsule n(SOD&CAT). Similarly, n(SOD) and n(CAT) were prepared in the same procedure.

The morphology of n(SOD&CAT), n(SOD) and n(CAT) capsules were observed by TEM analysis, which showed that all these capsules were monodisperse nanoparticles with uniform spherical shape ([Figure 1A](#) and [S1](#)). The hydrodynamic diameter and zeta potential values of n(SOD&CAT) were determined to  $24.38 \pm 7.35$  nm and  $+7.93 \pm 1.00$  mV, respectively ([Figure 1B](#)). The ideal size and zeta potential values were beneficial to facilitate the enzyme capsules to overcome the barrier of cell membrane and achieve the scavenging of intracellular ROS level. To verify whether n(SOD) and n(CAT) were successfully prepared, the n(SOD) and n(CAT) capsules were characterized through Coomassie-stained SDS-PAGE ([Figure S2](#)). Compared to native SOD and CAT, lag bands could be clearly observed for both n(SOD) and n(CAT) groups, indicating the successful construction of n(SOD) and n(CAT) capsules. These results indicated that we could achieve the preparation of n(SOD&CAT) capsules in the same procedure through the simultaneous addition of two components. To evaluate the stability of n(SOD) and n(CAT) in physiological fluids, the capsules were incubated in PBS (50 mM, pH 7.4) at room temperature, and the hydrodynamic diameter and zeta potential values were measured at predetermined time points ([Figure 1C](#) and [D](#)). The hydrodynamic diameter values of n(SOD) and n(CAT) were measured to be  $23.07 \pm 2.42$  and  $24.96 \pm 3.01$  nm, respectively, and did not change over time during the incubation in PBS for 5 days. Meanwhile, zeta potential values of n(SOD) and n(CAT) remained constant in the period ( $9.03 \pm 4.15$  and  $9.34 \pm$

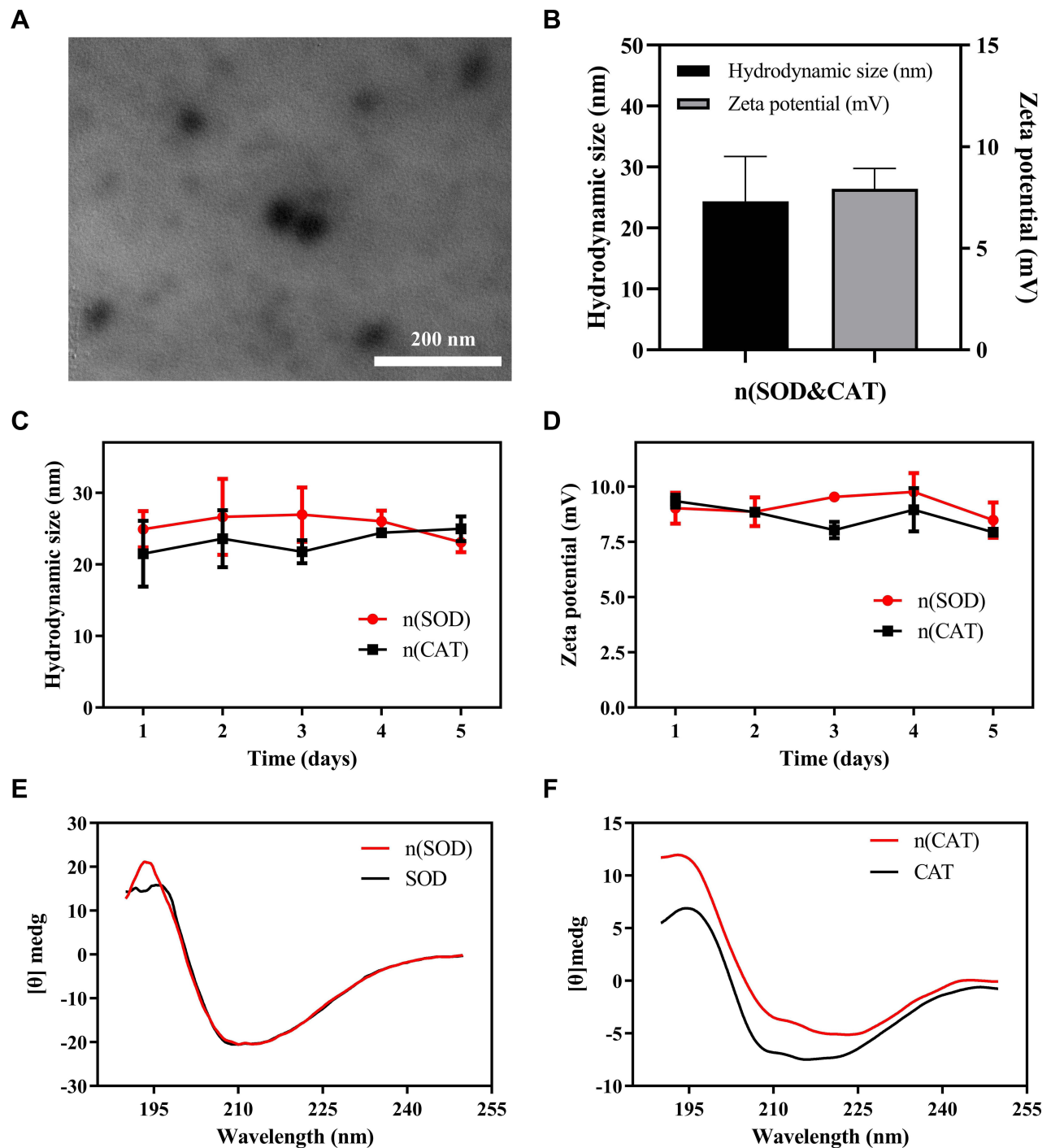


**Figure 1** (A) TEM image of n(SOD&CAT) capsules. (B) The hydrodynamic size and zeta potential of n(SOD&CAT) capsules. (C and D) The changes of hydrodynamic size and zeta potential of n(SOD) and n(CAT) capsules stored at room temperature within 5 days. (E and F) The CD spectra of native SOD, CAT, n(SOD) and n(CAT). Data were expressed as mean value  $\pm$  SD of triplicate experiments.

0.18 mV, respectively). All these results demonstrated the characteristic of excellent physiological stability of n(SOD) and n(CAT) capsules, which will be promising to obtain ideal delivery efficacy after the oral administration owing to the improved stability in the stomach and intestinal tract. Further, compared to native SOD and CAT, CD spectra of n(SOD) and n(CAT) showed no significant differences in the absorption of circularly polarized light (Figure 1E and F), indicating that the in situ polymerization did not affect the secondary structure of SOD and CAT which was beneficial to obtain

ideal catalytic activity. In comparison to native SOD and CAT, n(SOD) and n(CAT) capsules maintained 76.12% and 75.61% of initial catalytic activities with specific activity of  $2301.17 \pm 233.63$  and  $4998.49 \pm 1.78$  U/mg, respectively (Figure S3), demonstrating the introduction of polymeric shell on the enzymes' surface did not significantly block their catalytic activities.

Further, the stability of n(SOD) and n(CAT) capsules was evaluated in different incubation conditions. To assess the thermal stability, native SOD, CAT, n(SOD) and n(CAT) were incubated at 40 °C in PBS (50 mM, pH 7.4) for 24 h. As shown in Figure 2A, n(SOD) showed higher catalytic activity than native SOD during the incubation, especially for 8 and 24 h. n(SOD) could retain 76.27% of its original activity after the incubation for 24 h, while only 24.59% of enzymatic activity was maintained for native SOD. Similarly, n(CAT) exhibited significantly higher catalytic activity than native CAT after the incubation for 24 h (n(CAT) vs native CAT: 91.30% vs 41.83%) (Figure 2B). These findings indicated that the coating with polymeric shell around enzymes could remarkably improve the thermal stability of enzymes, which was useful for the long-term storage of enzyme formulations. To evaluate the proteolytic stability, native SOD, CAT, n(SOD) and n(CAT) were incubated with 50 µg/mL trypsin in PBS (50 mM, pH 7.4) at 37 °C for 30 min (Figure 2C and 2D). The activities of n(SOD) and n(CAT) were much stronger than those of native SOD and CAT after the treatment for 30 min (62.41% vs 29.61% for SOD, 51.16% vs 18.61% for CAT). Finally, the stability of enzyme formulations was studied under acidic conditions (pH 2.0). As shown in Figure 2E and 2F, both n(SOD) and n(CAT) exhibited higher activity than the native ones in acidic environment after the incubation for 4 h (87.68% vs 77.28% for n(SOD) and SOD, 90.33% and 56.37% for n(CAT) and CAT, respectively). These findings demonstrated that the encapsulation of enzymes in polymeric shells could protect proteins from the degradation by proteases and meanwhile obtain good resistance to the acidic conditions. Thus, the enzyme capsules could be potential to be used in the IBD treatment in an oral administration manner.

## ROS Scavenging Ability

To construct an efficient ROS scavenging system, SOD and CAT were co-encapsulated in polymeric shells to prepare n(SOD&CAT) capsule, and meanwhile n(SOD) and n(CAT) were mixed together to obtain n(SOD)+n(CAT) for the comparison. The ROS scavenging ability of different enzyme formulations toward •OH, H<sub>2</sub>O<sub>2</sub> and •O<sup>2-</sup>, was systematically evaluated to identify the potential elimination of representative ROS in intestinal inflammation. •OH is a representative ROS which can cause the damage to a variety of biomolecules in the body, but there are no specific enzymes to eliminate •OH.<sup>36</sup> Thus, the enzymes with •OH scavenging activity provided unique advantages in the elimination of ROS. The •OH scavenging activity of different enzyme formulations was evaluated (Figure S4A). The enzyme formulations harboring CAT showed similar •OH scavenging activity, which could achieve ca. 60% elimination of •OH. However, native SOD and n(SOD) did not possess the •OH scavenging activity, which was attributed to the fact that SOD reacted with •O<sup>2-</sup> specifically. Except for original H<sub>2</sub>O<sub>2</sub> in the inflamed sites, H<sub>2</sub>O<sub>2</sub> was also generated by •O<sup>2-</sup> dismutation under SOD. The H<sub>2</sub>O<sub>2</sub> scavenging efficiency of enzyme formulations was detected by H<sub>2</sub>O<sub>2</sub> assay kit. As shown in Figure S4B, the enzyme formulations containing CAT (CAT, n(CAT), SOD+CAT, n(SOD)+n(CAT) and n(SOD&CAT)) exhibited similar scavenging ability of H<sub>2</sub>O<sub>2</sub> with elimination ratio of 51–70%, while the decomposition of H<sub>2</sub>O<sub>2</sub> hardly happened for SOD and n(SOD). These results demonstrated that CAT could decompose H<sub>2</sub>O<sub>2</sub> into H<sub>2</sub>O and O<sub>2</sub> to relieve the oxidative stress. Finally, the •O<sup>2-</sup> scavenging ability of antioxidant enzymes was assayed by the hydroxylamine oxidation. As shown in Figure S4C, both SOD and n(SOD) showed significant •O<sup>2-</sup> scavenging ability with 73% of scavenging ratio. In contrast, the ability of •O<sup>2-</sup> scavenging for CAT and n(CAT) was much lower (<30%). Combination groups n(SOD)+n(CAT) and n(SOD&CAT) showed significant •O<sup>2-</sup> scavenging ability with elimination ratio of ca. 79%. The enzyme formulations containing SOD showed favorable •O<sup>2-</sup> scavenging ability, indicating the presence of SOD could specifically catalyze the dismutation of •O<sup>2-</sup>. Overall, the combination of SOD and CAT exhibited excellent scavenging activity toward all these representative ROS in the intestinal inflammation.

## Protection of Cells from the ROS-Induced Damage

The excellent ROS scavenging activity of n(SOD&CAT) capsule encouraged us to evaluate the cytoprotective effect at the cellular level, in which SW480 and HCT116 cells were employed as a model. First, the cytotoxicity of n(SOD) and

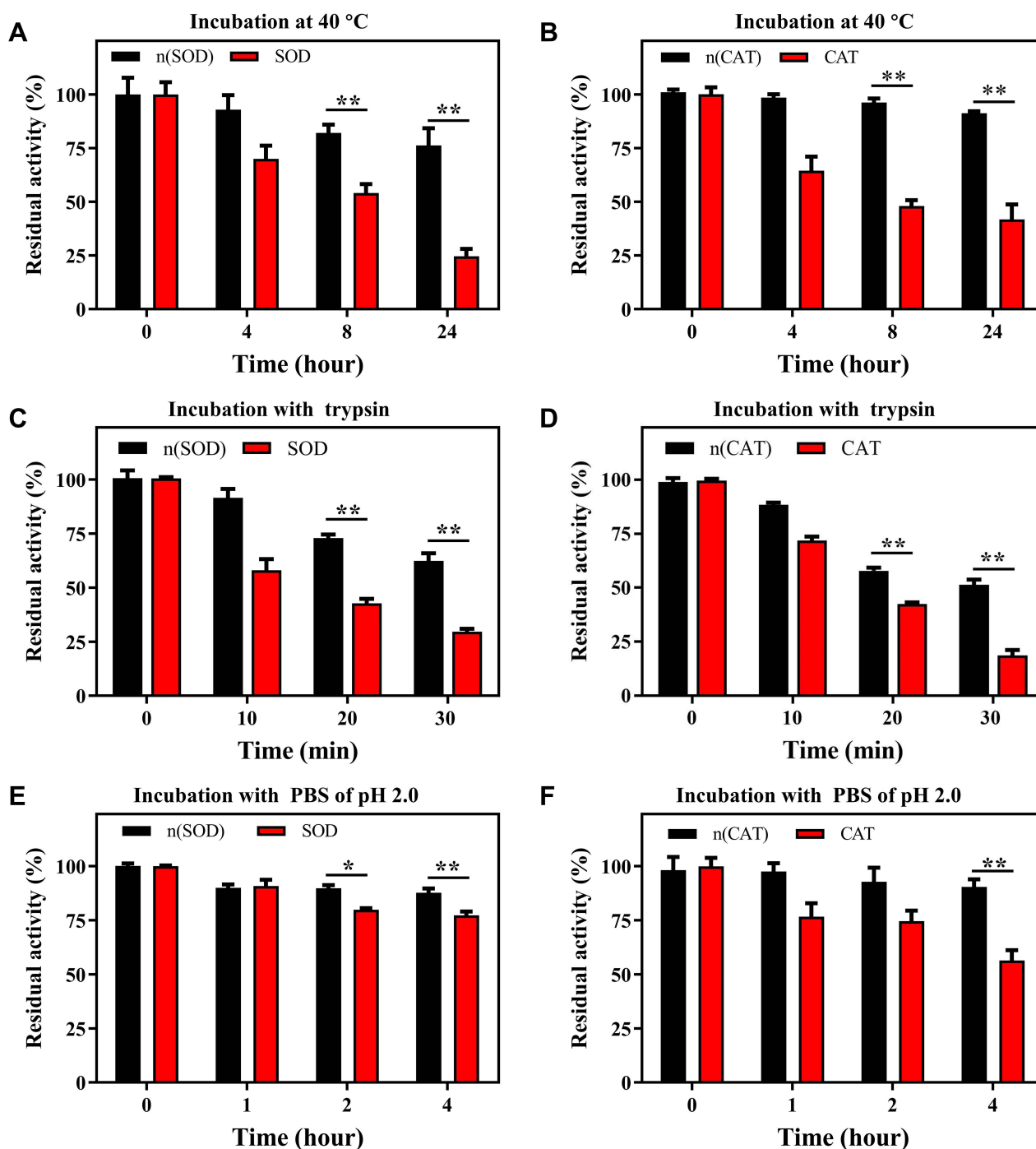


**Figure 2** The residual activities of SOD, CAT, n(SOD) and n(CAT) at predetermined time points after the incubation with PBS (50 mM, pH 7.4) at 40 °C within 24 h (A and B), 50 µg/mL trypsin in PBS (pH 7.4) at 37 °C within 30 min (C and D) and PBS (pH 2.0) at 37 °C within 4 h (E and F). Data were expressed as mean value ± SD of triplicate experiments. \**p* < 0.05 and \*\**p* < 0.01.

n(CAT) was evaluated by MTT assay (Figures S5 and S6). The viability of these two cells remained above 90% even with enzyme concentration up to 500 µg/mL, indicating that n(SOD) and n(CAT) capsules were favorably biocompatible. Subsequently, DCFH-DA was used as a fluorescent probe to monitor the intracellular ROS level through CLSM and flow cytometry. As shown in Figure S7, compared with the untreated SW480 cells, green fluorescence could be clearly observed after the treatment with Rosup though the cells have been pretreated with native enzymes (SOD, CAT and SOD +CAT), implying the improved intracellular ROS level in these groups. This phenomenon was caused by that free



enzymes could not overcome the barrier of cell membrane and facilitate the intracellular ROS scavenging. The intensity of green fluorescence decreased significantly when the cells were preincubated with n(SOD), n(CAT), n(SOD)+n(CAT) and n(SOD&CAT), as shown in [Figure 3](#). These results were attributed to the fact that the introduction of cationic polymeric shells could facilitate the cellular uptake of enzyme capsules, thereby eliminating the intracellular ROS. In addition, the combination of n(SOD) and n(CAT) could achieve higher ROS scavenging activity than the single components, attributing to the stronger scavenging ability for different types of ROS mediated by n(SOD)+n(CAT) and n(SOD&CAT). Meanwhile, the intracellular ROS level was examined by flow cytometry, and the results were consistent with CLSM images ([Figure S8](#)). The intracellular ROS level increased 4.75-fold after the Rosup treatment, while it changed to 2.27- and 2.04-fold when the cells were pretreated with n(SOD)+n(CAT) and n(SOD&CAT). In addition, the intracellular ROS level decreased with the improvement of n(SOD&CAT) concentration (0–15  $\mu\text{g/mL}$ ), indicating that n(SOD&CAT) capsule could dose-dependently execute the ROS scavenging activity ([Figure S9](#)). Moreover, the ROS scavenging ability of enzyme capsules was performed after the pretreatment in KCl-HCl solution (pH 2.0) for 2 h through flow cytometry. As shown in [Figure S10](#), compared with the unpretreated groups, the pretreatment in KCl-HCl solution caused slight decrease in the ROS scavenging ability of enzyme capsules. The results

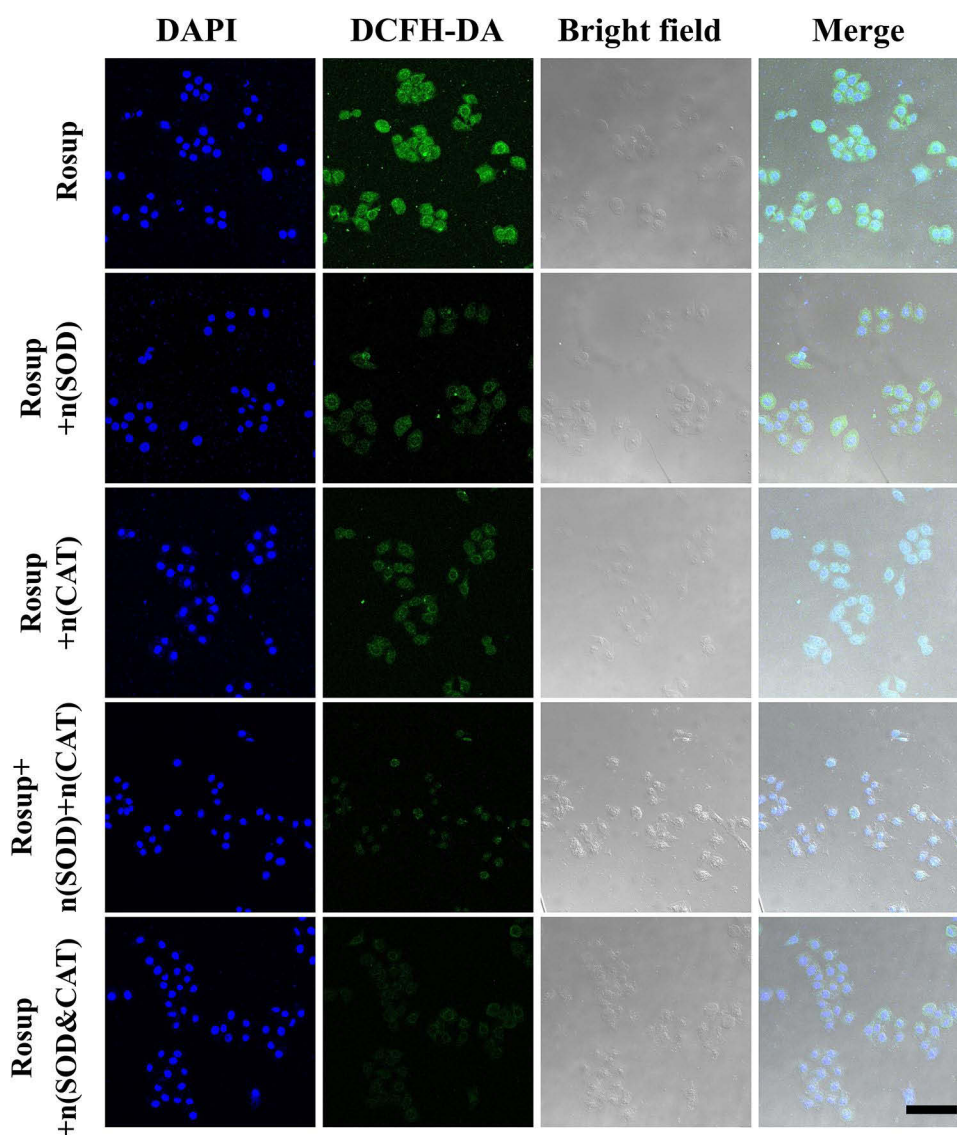


**Figure 3** CLSM images of SW480 cells with the treatment of Rosup (1 mg/mL), in which the cells were preincubated with n(SOD), n(CAT), n(SOD)+n(CAT) and n(SOD&CAT) for 6 h (SOD: 5  $\mu\text{g/mL}$ ; CAT: 10  $\mu\text{g/mL}$ ). Nucleus and ROS were stained with DAPI (blue) and DCFH-DA (green), respectively. The scale bar is 50  $\mu\text{m}$ .

revealed that the enzyme capsules could maintain good activity and stability under acidic conditions, providing an ideal foundation for the oral administration of proteins. Finally, the cytoprotective ability of different formulations against the Rosup-induced oxidative stress was investigated in SW480 and HCT116 cells (Figure S11). As anticipated, the Rosup treatment could obviously induce the cell death owing to the improvement of intracellular ROS level, whereas the formulations n(SOD), n(CAT), n(SOD)+n(CAT) and n(SOD&CAT) could attenuate the oxidative stress-induced cell death. The n(SOD&CAT) capsule exhibited higher protection ability against the oxidative stress than the single components with cell viability of ca. 84.0% in these two cells. Overall, the enzyme capsules could be used as effective ROS scavengers to protect the cells from the oxidative stress-induced damage.

## In vitro Anti-Inflammation Analysis

To further study the anti-inflammatory activity of different formulations, the expressions of key pro-inflammatory cytokines were analyzed by qPCR using macrophages RAW264.7 as a model. Generally, LPS was used to polarize macrophages RAW264.7 to the M1 phenotype, and the expression of pro-inflammatory cytokines (IL-6, TNF- $\alpha$  and CCL2) was upregulated compared with the untreated cells.<sup>37,38</sup> Herein, the qPCR analysis revealed that 3.3-, 10.0- and 3.2-fold improvement could be achieved in the mRNA levels of IL-6, TNF- $\alpha$  and CCL2 after the LPS treatment, respectively (Figure 4). Meanwhile, there were no significant differences in the mRNA levels of IL-6, TNF- $\alpha$  and CCL2 between the treatment with native enzymes (SOD, CAT and SOD+CAT) and the LPS-induced group with no treatment, owing to the weak internalization of these free enzymes. In contrast, the cells after the treatment with enzyme capsules n(SOD) and n(CAT) resulted in significantly lower mRNA level of pro-inflammatory factors than those of native enzymes. More importantly, the combination groups n(SOD)+n(CAT) and n(SOD&CAT) could inhibit the production of pro-inflammatory factors more significantly than n(SOD) and n(CAT) capsules through the cascade catalysis mediated by these two enzymes. These results clearly demonstrated that the in situ polymerization around enzyme molecules was necessary to achieve the in vitro anti-inflammation of enzyme formulations.

## Ex vivo Biodistribution Analysis

To study the intestinal distribution of native and encapsulated enzymes, C57BL/6N mice were used to construct the DSS-induced colitis model and then subjected to the ex vivo imaging study. The dye RBITC-labelled enzymes RBITC-SOD and n(RBITC-SOD) were orally administrated at a dose of 5 mg/kg. At predetermined time intervals (2, 4 and 12 h) after the oral administration, the mice were euthanized, and colons and other major organs were excised and imaged (Figure 5). There were no obvious differences in the fluorescence intensity at the colonic tissues of DSS-induced colitis mice between RBITC-SOD and n(RBITC-SOD) at 2 and 4 h after the oral administration of these two enzymes. However, the DSS-induced colitis mice treated with n(RBITC-SOD) showed significantly higher fluorescence in the colon tissues at 12 h post oral administration. Quantitative analysis revealed that the fluorescence intensity in the colon

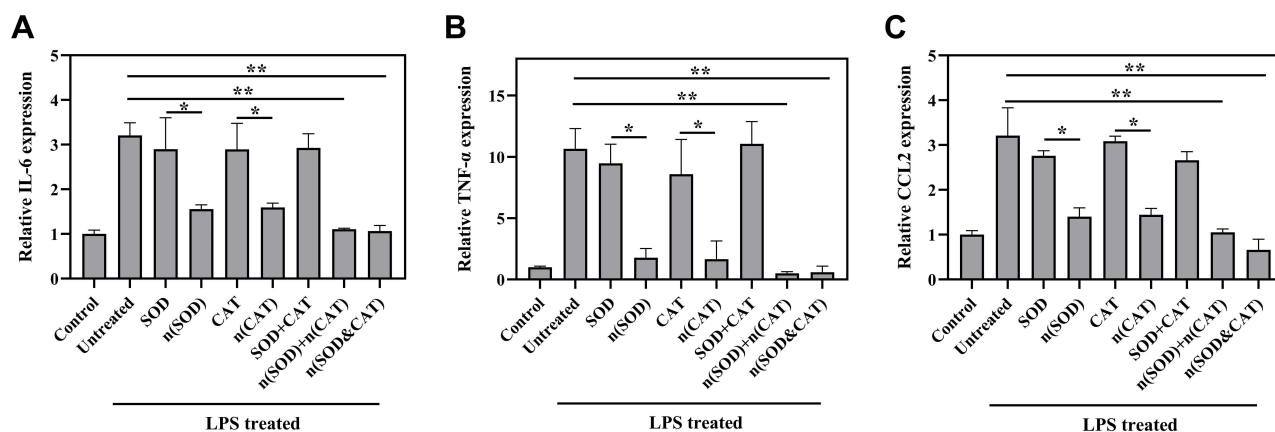


**Figure 4** The mRNA levels of pro-inflammatory cytokines IL-6 (A), TNF- $\alpha$  (B) and CCL2 (C) in the LPS-induced macrophages RAW 264.7 after the treatment with different formulations. Data were expressed as mean  $\pm$  SD of triplicate experiments (\* $p$  < 0.05 and \*\* $p$  < 0.01).

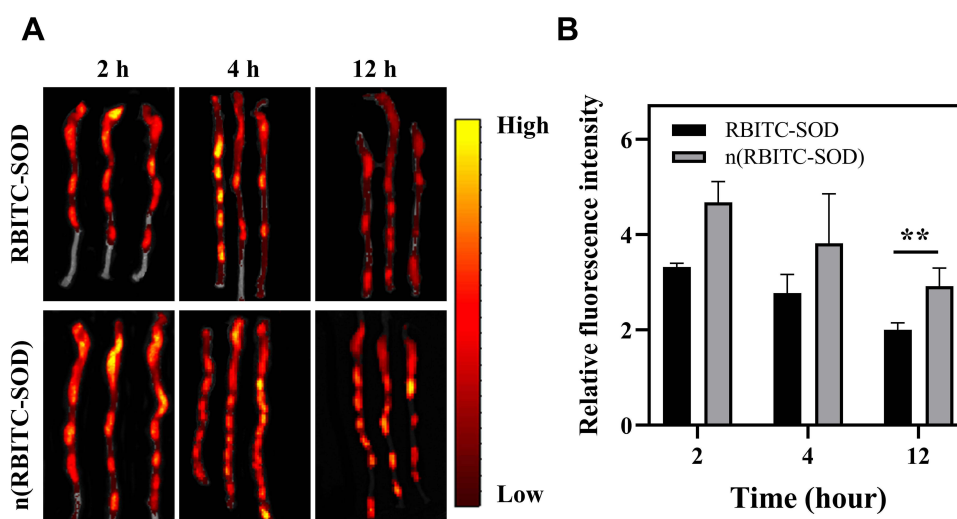


**Figure 5** Representative ex vivo fluorescence images (A) and quantitative analysis (B) of colons in DSS-induced colitis mice at 2, 4 and 12 h after the oral administration of RBITC-SOD or n(RBITC-SOD). Data were expressed as mean  $\pm$  SD of triplicate experiments (\*\* $p < 0.01$ ).

tissues of n(RBITC-SOD)-treated mice was 1.4-fold higher than that of RBITC-SOD-treated mice. In addition, the accumulation of n(RBITC-SOD) in major organs (heart, liver, spleen, lung and kidney) was much lower than in the colon tissues (Figure S12). Strong fluorescence could be observed in the stomach, which was correlated with the route of oral administration. These results indicated that the enzyme capsules were beneficial to improve the distribution of enzyme molecules in the inflamed colons owing to the protective effect of polymeric shell against the complex conditions in the body. Meanwhile, the long-term distribution of n(RBITC-SOD) in colon tissues was favorable to obtain ideal therapeutic efficacy for the IBD treatment. Finally, the fluorescence intensity in the liver was almost identical for these two groups, which was probably caused by the fact that the in situ polymerization only enhanced the stability of enzymes but did not change the inherent metabolic profile of enzyme molecules.

## Therapeutic Efficacy Analysis in DSS-Induced Colitis Mice

The favorable anti-inflammation ability and effective accumulation in colon tissues of enzyme capsules provided a rationale to evaluate the efficacy in the treatment of DSS-induced colitis. The C57BL/6N mice were fed with 3% DSS in drinking water from Day 1 for 7 days to establish a colitis model, and the therapeutic enzyme formulations were orally administered on Day 1, 3, 5 and 7 for 4 times (Figure 6A). Meanwhile, the healthy mice were used as negative control. Significant decrease in body weight could be clearly observed in the DSS-induced mice after the saline treatment, and the administration of SOD+CAT could not relieve the loss of body weight owing to the degradation of enzyme molecules in the digestive tract (Figure 6B). However, both n(SOD)+n(CAT) and n(SOD&CAT) could significantly reduce the loss of body weight. The photographs of colon tissues and the colon length measurement showed that the colons of n(SOD)+n(CAT) and n(SOD&CAT) treatment groups (5.85 and 6.33 cm, respectively) were significantly longer than the group of saline treatment (5.38 cm), as shown in Figure 6C and D). Additionally, the colon length of SOD+CAT-treated mice showed no significant differences compared with the saline treatment group. These results further verified the favorable therapeutic efficacy of enzyme capsules for the IBD in an oral administration manner. Further, the index of spleen in n(SOD)+n(CAT) and n(SOD&CAT) groups decreased in comparison to the saline and SOD+CAT treatment groups (Figure 6E). Since the spleen is an important immune organ, these results meant that the oral administration of n(SOD)+n(CAT) and n(SOD&CAT) could suppress the inflammatory response in vivo. For the index of heart, liver, lung and kidney, there were no significant differences between the healthy mice and the treatment groups, which was consistent with lower accumulation of enzyme capsules in these tissues (Figure S13). The severity of inflammation was further assessed by DAI scores, including weight loss, bloody stool and stool consistency. As shown in Figure 6F, the DSS-induced colitis mice after the treatment with saline showed the highest DAI value (10.67), indicating

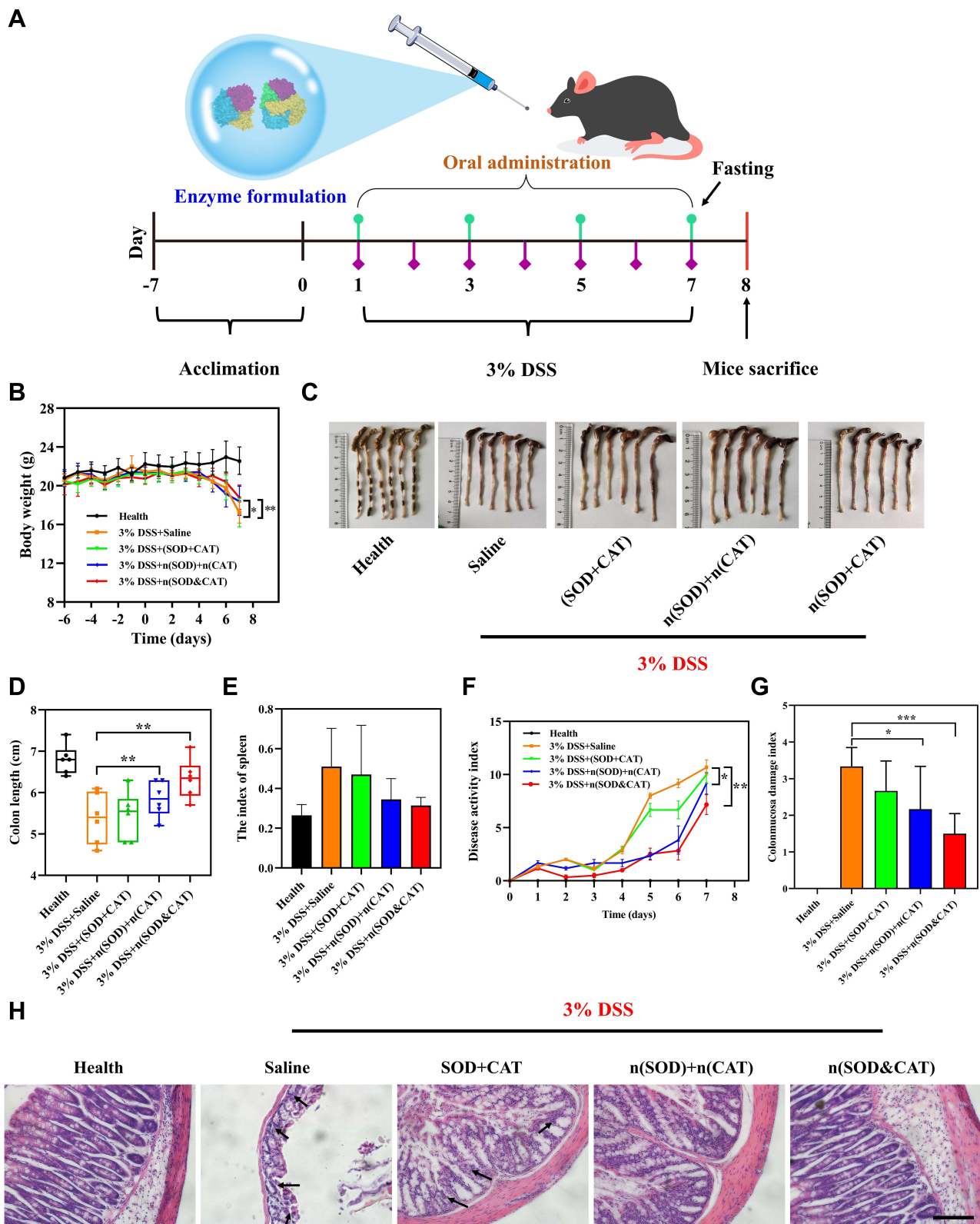


**Figure 6** (A) Schematic illustration of the experimental procedure. C57BL/6N mice were fed with water or 3% DSS-containing water for 7 days, and the mice were orally administered with different enzyme formulations every other day at a dose of 3 mg/kg for SOD and 6 mg/kg for CAT ( $n=6$  per group). (B) Body weight changes during the experiment. (C and D) Photographs and length of the colons on Day 8. (E) The index of spleen after the treatment with different formulations. (F) Changes in DAI, which is the summation of fecal consistency index (0–4), fecal bleeding index (0–4) and weight loss index (0–4). (G) CDMI scores after the treatment with different formulations. (H) H&E staining of colonic pathological sections in the mice after the treatment with different formulations on Day 8 (scale bar: 200  $\mu$ m), in which mucosal damage or inflammatory infiltration were marked with arrows. Data were expressed as mean  $\pm$  SD (\* $p < 0.05$ , \*\* $p < 0.01$  and \*\*\* $p < 0.001$ ).



DSS could induce severe *in vivo* inflammation. The administration of n(SOD)+n(CAT) and n(SOD&CAT) could dramatically decrease the DAI values during the experiment (9.17 and 7.17 for these two groups), indicating the obvious anti-inflammation effect of these capsules. Clearly, the n(SOD&CAT) capsule exhibited lower DAI values than the n(SOD)+n(CAT) group, mainly attributing to the synergistic manner in the ROS scavenging of the co-encapsulated enzymes. The photographs of rectal areas also showed serious inflammation with bloody rectal areas in the DSS-induced colitis mice after the treatment with saline and SOD+CAT (Figure S14). Nevertheless, the administration of n(SOD)+n(CAT) and n(SOD&CAT) resulted in significantly suppressed inflammation with lower DAI values and obviously relieved inflammation in the rectal areas. These results were consistent with the CDMI scores for assessing colonic lesions, including adhesions, strictures, ulcers and wall thickness (Figure 6G). To further validate the therapeutic efficacy of enzyme capsules, the excised colon was subjected to the H&E staining, in which mucosal damage or inflammatory infiltration were marked with arrows (Figure 6H). The colon of DSS-induced colitis mice showed significant loss of structural integrity of the colon, disruption of crypt glands, and damage of the mucosal surface in comparison to the colon tissues of healthy mice. The administration of SOD+CAT showed slight therapeutic effect, which was mainly caused by the incomplete degradation of SOD and CAT. Notably, the treatment with n(SOD)+n(CAT) and n(SOD&CAT) capsules showed significantly ungraded mucosal structure. All these results clearly suggested that the oral administration of encapsulated enzymes possessed the ability to improve the therapeutic efficacy of DSS-induced colitis mice, owing to the ROS scavenging and anti-inflammation effects.

## Therapeutic Mechanism Analysis

To discuss the therapeutic mechanism of different formulations in DSS-induced colitis mice, ROS level, SOD activity, CAT activity, MPO activity and MDA content in colon tissues were measured. The ROS level in colon tissue was measured using DCFH-DA probe by flow cytometry. As shown in Figure 7A and B, the ROS level in colon tissues significantly increased in the DSS-induced colitis mice in comparison to the healthy mice, and the administration of SOD+CAT could not reduce the ROS level. In contrast, ROS levels significantly decreased after the treatment with n(SOD)+n(CAT) and n(SOD&CAT) capsules, indicating the encapsulated enzyme formulations were highly effective in scavenging ROS in the inflamed colons. The SOD or CAT activity after the treatment with SOD+CAT was slightly improved compared with the saline-treated group, further demonstrating the native enzymes could maintain limited residual activity after the oral administration (Figure 7C and D). Remarkably, the oral administration of n(SOD)+n(CAT) and n(SOD&CAT) exhibited much higher SOD (0.31 and 0.32 U/mg tissue for these two groups) and CAT activities (21.95 and 26.01 U/mg tissue for these two groups), which provided a favorable foundation for the ideal therapeutic efficacy of enzyme capsules in the IBD treatment. There were two probable reasons for the enhanced SOD and CAT activities in the colon tissues: (1) the polymeric shell of encapsulated enzyme formulations could protect the enzymes from undesirable degradation to maintain high enzymatic activity after the oral administration; and (2) the encapsulated enzyme formulations showed higher accumulation in the colon tissues. Furthermore, the levels of MDA and MPO in colons were measured to assess the colon injury. MDA is an important indicator of lipid peroxidation to assess oxidative damage,<sup>39</sup> and MPO is a glycolytic enzyme located in neutrophils and interstitial cells which can be used as a biomarker to assess the disease status of patients with IBD.<sup>40</sup> As shown in Figure 7E and F, both MDA and MPO have been significantly upregulated in the colon tissues of DSS-induced colitis mice, and the administration of n(SOD&CAT) and n(SOD)+n(CAT) could remarkably inhibit the levels of these two indicators, especially for the n(SOD&CAT) group (94.60 pmol/mg tissue for MDA and 0.21 U/g tissue for MPO). Meanwhile, compared to n(SOD&CAT) and n(SOD)+n(CAT), SOD+CAT was less effective in the IBD therapy due to the instability and short half-life of natural enzymes in the gastrointestinal tract. After the *in situ* polymerization around enzyme molecules, the polymeric shell could enhance the stability and half-life of enzymes, thereby obtaining higher elimination ability for excess ROS to achieve an ideal therapeutic purpose.

To further investigate the anti-inflammation mechanism of enzyme formulations in the DSS-induced colitis model, the expression of pro-inflammatory cytokines (IL-6, TNF- $\alpha$  and CCL2) in colon tissues were evaluated using qPCR and ELISA assays. As shown in Figure 8A–C, the expression of IL-6, TNF- $\alpha$  and CCL2 were significantly upregulated in the DSS-induced colitis mice, and the saline treatment did not influence the levels of these cytokines. Notably, the expression



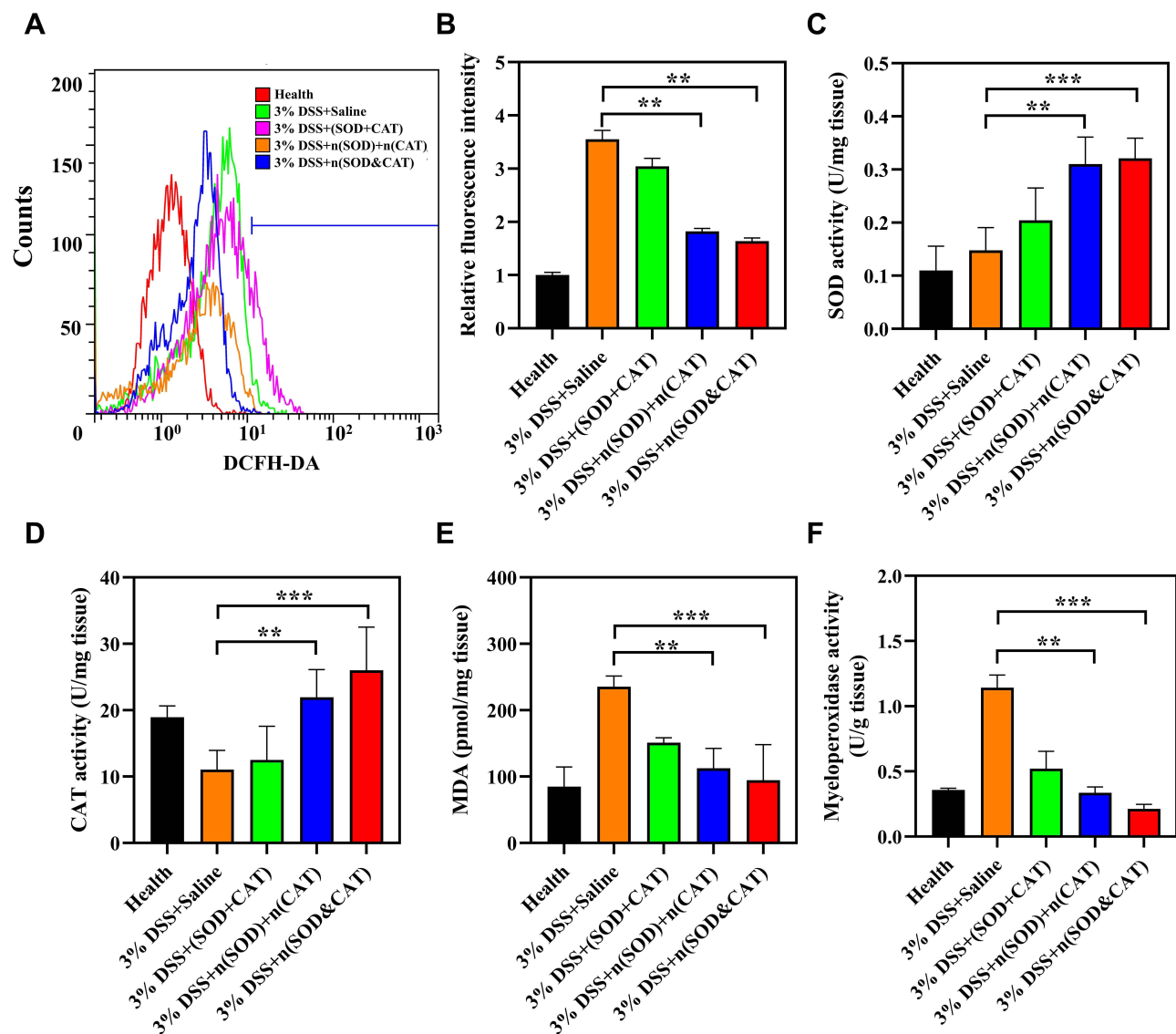


**Figure 7** (A and B) Flow cytometry and quantitative analysis of the ROS level in colon tissues using DCFH-DA probe. (C–F) The SOD activity, CAT activity, MDA content and MPO activity in the colon tissues after the treatment with different formulations ( $n=6$  per group). Data were presented as mean  $\pm$  SD (\*\* $p < 0.01$  and \*\*\* $p < 0.001$  vs the saline group).

levels of pro-inflammatory cytokines IL-6, TNF- $\alpha$  and CCL2 have been significantly inhibited after the oral administration of n(SOD)+n(CAT) and n(SOD&CAT). The treatment with SOD+CAT also showed decreased level of TNF- $\alpha$ , which was mainly caused by the incomplete digestion of SOD and CAT molecules in the gastrointestinal tract. The ELISA assay for the contents of these cytokines showed the same pattern as the qPCR analysis (Figure 8D–F). The contents of cytokines IL-6, TNF- $\alpha$  and CCL2 after the treatment with n(SOD&CAT) capsule were determined to be 17.91, 39.69 and 437.81 pg/mg tissue, respectively. All these results demonstrated that the initiation of in situ polymerization on the surface of proteins could effectively stabilize enzyme molecules and prevent the degradation in the gastrointestinal tract after the oral administration. Thus, the accumulation of enzyme agents in the intestine could eliminate excess ROS, relieve oxidative stress in colon cells, and suppress inflammation by regulating the infiltration of neutrophils and the secretion of pro-inflammatory cytokines.

## Biosafety Evaluation

As safety is always the top priority, the in vivo toxicity of enzyme formulations was further studied to evaluate the clinical potential as anti-inflammation agents after the oral administration. The liver function-related blood biochemical

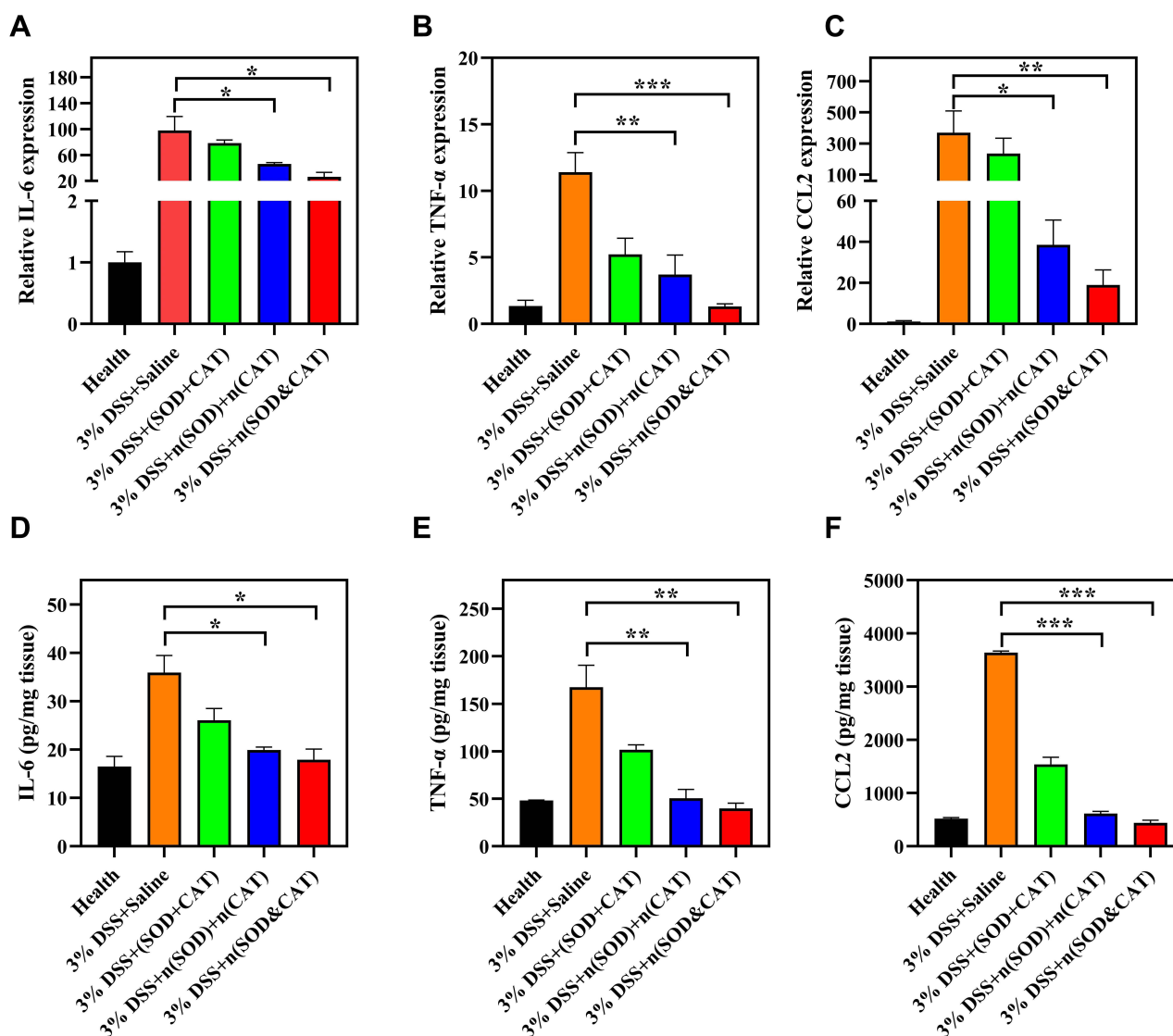


**Figure 8 (A–C)** qPCR and **(D–F)** ELISA analysis of pro-inflammatory cytokines (IL-6, TNF- $\alpha$  and CCL2) in the colon tissues of DSS-induced colitis mice after the treatment with different formulations (n=6 per group). Data were presented as mean  $\pm$  SD (\* $p$  < 0.05, \*\* $p$  < 0.01 and \*\*\* $p$  < 0.001 vs the saline group).

values (ALT, AST and ALP) as well as the kidney function-related blood biochemical values (BUN and CREA) in the serum of mice on Day 8 were assayed to evaluate the effects of enzyme capsules on the liver and kidney functions. As shown in [Figure S15](#), compared to the healthy mice, no significant differences have been found in the mice after the treatment with enzyme formulations, suggesting that no liver and kidney function damage was caused by enzyme formulations. It was also noteworthy that no obvious tissue damages happened after the treatment with enzyme formulations in the H&E staining of major organs (heart, liver, spleen, lung and kidney), as shown in [Figure S16](#). All these results indicated that the encapsulated enzyme formulations possessed excellent biosafety and biocompatibility, thereby providing great potential as a candidate in the IBD treatment.

## Conclusion

In conclusion, a strategy based on protein surface-initiated in situ polymerization has been successfully established to encapsulate the antioxidant enzymes SOD and CAT for oral delivery, in which the polymeric shell of enzyme capsules could protect the enzymes from the degradation under acidic conditions. The treatment with n(SOD)+n(CAT) or n(SOD&CAT) capsules were effective in scavenging the intracellular ROS, protecting cells from the ROS-induced

oxidative damage and inhibiting the expression of pro-inflammatory cytokines. Meanwhile, the enzyme capsules exhibited higher accumulation ability in the inflamed colon tissues than native enzymes after the oral administration in DSS-induced colitis mice. Moreover, the oral delivery of n(SOD&CAT) capsule could effectively alleviate the symptoms associated with colitis, attributing to the excellent ROS scavenging ability and the inhibition of pro-inflammatory cytokines' level in the colon tissues. Overall, this strategy provided a promising oral nano-delivery system of therapeutic enzymes, and thus opened a new avenue for promoting the antioxidant enzymes-based therapy in the inflammatory diseases.

## Acknowledgments

The work was supported by National Key R&D Program of China (2020YFA0907003), National Natural Science Foundation of China (32071267 and 81872928), Development and Reform Commission of Jilin Province (2021C041-4) and Interdisciplinary Innovation Program of Jilin University (JLUXKJC2020308).

## Disclosure

The authors report no conflicts of interest in this work.

## References

1. Abraham C, Cho JH. Inflammatory bowel disease. *N Engl J Med*. 2009;361:2066–2078. doi:10.1056/NEJMra0804647
2. Gergely M, Prado E, Deepak P. Management of refractory inflammatory bowel disease. *Curr Opin Gastroenterol*. 2022;38:347–357. doi:10.1097/MOG.0000000000000849
3. Ananthakrishnan N. Epidemiology and risk factors for IBD. *Nat Rev Gastroenterol Hepatol*. 2015;12:205–217. doi:10.1038/nrgastro.2015.34
4. Khor B, Gardet A, Xavier RJ. Genetics and pathogenesis of inflammatory bowel disease. *Nature*. 2011;474:307–317. doi:10.1038/nature10209
5. Zhang M, Sun K, Wu Y, et al. Interactions between intestinal microbiota and host immune response in inflammatory bowel disease. *Front Immunol*. 2017;8:942. doi:10.3389/fimmu.2017.00942
6. Singh A, Kaur K, Kaur V, et al. Importance of nanocarriers and probiotics in the treatment of ulcerative colitis. *J Drug Deliv Therapeut*. 2019;9:216–228. doi:10.22270/jddt.v9i6-s.3727
7. Singh A, Kaur K, Mandal UK, et al. Nanoparticles as budding trends in colon drug delivery for the management of ulcerative colitis. *Curr Nanomed*. 2020;10:225–247. doi:10.2174/2468187310999200621200615
8. Yang J, Zhou J, Zhao Y, et al. Hollow CeO<sub>2</sub> with ROS-scavenging activity to alleviate colitis in mice. *Int J Nanomedicine*. 2021;16:6889–6904. doi:10.2147/IJN.S317261
9. Tian T, Wang Z, Zhang J. Pathomechanisms of oxidative stress in inflammatory bowel disease and potential antioxidant therapies. *Oxidative Med Cell Longev*. 2017;2017:4535194. doi:10.1155/2017/4535194
10. Zhang S, Ermann J, Succu MD, et al. An inflammation-targeting hydrogel for local drug delivery in inflammatory bowel disease. *Sci Transl Med*. 2015;7:300ra128. doi:10.1126/scitranslmed.aaa5657
11. Lee YH, Sugihara K, Gilliland MG, et al. Hyaluronic acid-bilirubin nanomedicine for targeted modulation of dysregulated intestinal barrier, microbiome and immune responses in colitis. *Nat Mater*. 2020;19:118–126. doi:10.1038/s41563-019-0462-9
12. Zeng Z, He X, Li C, et al. Oral delivery of antioxidant enzymes for effective treatment of inflammatory disease. *Biomaterials*. 2021;271:120753. doi:10.1016/j.biomaterials.2021.120753
13. Li S, Xie A, Li H, et al. A self-assembled, ROS-responsive Janus-prodrug for targeted therapy of inflammatory bowel disease. *J Control Release*. 2019;316:66–78. doi:10.1016/j.jconrel.2019.10.054
14. Lin Y, Chen Y, Liu T, et al. Approach to deliver two antioxidant enzymes with mesoporous silica nanoparticles into cells. *ACS Appl Mater Interfaces*. 2016;8:17944–17954. doi:10.1021/acsami.6b05834
15. Andrabi SS, Yang J, Gao Y, et al. Nanoparticles with antioxidant enzymes protect injured spinal cord from neuronal cell apoptosis by attenuating mitochondrial dysfunction. *J Control Release*. 2020;317:300–311. doi:10.1016/j.jconrel.2019.12.001
16. Dong Y, Zhuang H, Hao Y, et al. Poly(N-isopropyl-acrylamide)/poly(γ-glutamic acid) thermo-sensitive hydrogels loaded with superoxide dismutase for wound dressing application. *Int J Nanomedicine*. 2020;15:1939–1950. doi:10.2147/IJN.S235609
17. Fukai T, Fukai MU. Superoxide dismutases: role in redox signaling, vascular function, and diseases. *Antioxid Redox Signal*. 2011;15:1583–1606. doi:10.1089/ars.2011.3999
18. Weydert CJ, Cullen JJ. Measurement of superoxide dismutase, catalase and glutathione peroxidase in cultured cells and tissue. *Nat Protoc*. 2010;5:51–66. doi:10.1038/nprot.2009.197
19. Ren X, Chen D, Wang Y, et al. Nanozymes-recent development and biomedical applications. *J Nanobiotechnol*. 2022;20:92. doi:10.1186/s12951-022-01295-y
20. Wei XL, Gastelum MB, Karshalev E, et al. Biomimetic micromotor enables active delivery of antigens for oral vaccination. *Nano Lett*. 2019;19:1914–1921. doi:10.1021/acs.nanolett.8b05051
21. Xu W, Ling P, Zhang T. Polymeric micelles, a promising drug delivery system to enhance bioavailability of poorly water-soluble drugs. *J Drug Deliv*. 2013;2013:340315. doi:10.1155/2013/340315
22. Liu L, Yao W, Rao Y, et al. pH-Responsive carriers for oral drug delivery: challenges and opportunities of current platforms. *Drug Deliv*. 2017;24:569–581. doi:10.1080/10717544.2017.1279238

23. Zhou Y, Chen Z, Zhao D, et al. A pH-triggered self-unpacking capsule containing zwitterionic hydrogel-coated MOF nanoparticles for efficient oral Exendin-4 delivery. *Adv. Mater.* **2021**;33:2102044. doi:10.1002/adma.202102044
24. Zeng Z, Qi D, Yang L, et al. Stimuli-responsive self-assembled dendrimers for oral protein delivery. *J Control Release.* **2019**;315:206–213. doi:10.1016/j.jconrel.2019.10.049
25. Bizeau J, Mertz D. Design and applications of protein delivery systems in nanomedicine and tissue engineering. *Adv Colloid Interface Sci.* **2021**;287:102334. doi:10.1016/j.cis.2020.102334
26. Zhou Y, Liu L, Cao Y, et al. A nanocomposite vehicle based on metal-organic framework nanoparticle incorporated biodegradable microspheres for enhanced oral insulin delivery. *ACS Appl Mater Interfaces.* **2020**;12:22581–22592. doi:10.1021/acsami.0c04303
27. Jia X, Wang L, Du J. In situ polymerization on biomacromolecules for nanomedicines. *Nano Res.* **2018**;11:5028–5048. doi:10.1007/s12274-018-2080-2
28. Pelegri-O'Day E, Lin E, Maynard H. Therapeutic protein-polymer conjugates: advancing beyond PEGylation. *J Am Chem Soc.* **2014**;136:14323–14332. doi:10.1021/ja504390x
29. Liang S, Liu Y, Jin X, et al. Phosphorylcholine polymer nanocapsules prolong the circulation time and reduce the immunogenicity of therapeutic proteins. *Nano Res.* **2016**;9:1022–1031. doi:10.1007/s12274-016-0991-3
30. Yan M, Du J, Gu Z, et al. A novel intracellular protein delivery platform based on single-protein nanocapsules. *Nat Nanotechnol.* **2010**;5:48–53. doi:10.1038/nnano.2009.341
31. Ilochonwu BC, Urtti A, Hennink WE, et al. Intravitreal hydrogels for sustained release of therapeutic proteins. *J Control Release.* **2020**;326:419–441. doi:10.1016/j.jconrel.2020.07.031
32. Qin M, Cao Z, Wen J, et al. An antioxidant enzyme therapeutic for COVID-19. *Adv Mater.* **2020**;32:2004901. doi:10.1002/adma.202004901
33. Hu J, Wang Q, Wang Y, et al. Polydopamine-based surface modification of hemoglobin particles for stability enhancement of oxygen carriers. *J Colloid Interface Sci.* **2020**;571:326–336. doi:10.1016/j.jcis.2020.03.046
34. Chen W, Liu Y, Liang X, et al. Chondroitin sulfate-functionalized polyamidoamine as a tumor-targeted carrier for miR-34a delivery. *Acta Biomater.* **2017**;57:238–250. doi:10.1016/j.actbio.2017.05.030
35. Luk HH, Ko JKS, Fung HS, et al. Delineation of the protective action of zinc sulfate on ulcerative colitis in rats. *Eur. J. Pharmacol.* **2020**;443:197–204. doi:10.1016/S0014-2999(02)01592-3
36. Dandona P, Thusu K, Cook S, et al. Oxidative damage to DNA in diabetes mellitus. *Lancet.* **1996**;347:444. doi:10.1016/S0140-6736(96)90013-6
37. Kesharwani SS, Ahmad R, Bakkari MA, et al. Site-directed non-covalent polymer-drug complexes for inflammatory bowel disease (IBD): formulation development, characterization and pharmacological evaluation. *J Control Release.* **2018**;290:165–179. doi:10.1016/j.jconrel.2018.08.004
38. Zhang J, Zhao Y, Hou T, et al. Macrophage-based nanotherapeutic strategies in ulcerative colitis. *J Control Release.* **2020**;320:363–380. doi:10.1016/j.jconrel.2020.01.047
39. Kadikoylu G, Yazak V, Yenisey C, et al. Role of reactive oxygen species and lipid peroxidation in patients with newly diagnosed hematological malignancies. *Blood.* **2011**;118:5199. doi:10.1182/blood.V118.21.5199.5199
40. Dos Santos AM, Carvalho SG, Menefuin AB, et al. Oral delivery of micro/nanoparticulate systems based on natural polysaccharides for intestinal diseases therapy: challenges, advances and future perspectives. *J Control Release.* **2021**;10:353–366. doi:10.1016/j.jconrel.2021.04.026

## International Journal of Nanomedicine

Dovepress

### Publish your work in this journal

The International Journal of Nanomedicine is an international, peer-reviewed journal focusing on the application of nanotechnology in diagnostics, therapeutics, and drug delivery systems throughout the biomedical field. This journal is indexed on PubMed Central, MedLine, CAS, SciSearch®, Current Contents®/Clinical Medicine, Journal Citation Reports/Science Edition, EMBase, Scopus and the Elsevier Bibliographic databases. The manuscript management system is completely online and includes a very quick and fair peer-review system, which is all easy to use. Visit <http://www.dovepress.com/testimonials.php> to read real quotes from published authors.

Submit your manuscript here: <https://www.dovepress.com/international-journal-of-nanomedicine-journal>